Digital Color Image Processing
by Andreas Koschan and Mongi Abidi

3 COLOR SPACES AND COLOR DISTANCES

Color is a perceived phenomenon and not a physical dimension like length or temperature, although the electromagnetic radiation of the visible wavelength spectrum is measurable as a physical quantity. The observer can perceive two differing color sensations wholly as equal or as metameric (see Section 2.2). Color identification through data of a spectrum is not useful for labeling colors that, as also in image processing, are physiologically measured and evaluated for the most part with a very small number of sensors. A suitable form of representation must be found for storing, displaying, and processing color images. This representation must be well suited to the mathematical demands of a color image processing algorithm, to the technical conditions of a camera, printer, or monitor, and to human color perception as well. These various demands cannot be met equally well simultaneously. For this reason, differing representations are used in color image processing according to the processing goal.

Color spaces indicate *color coordinate systems* in which the image values of a color image are represented. The difference between two image values in a color space is called *color distance*. The numbers that describe the different color distances in the respective color model are as a rule not identical to the color differences perceived by humans. In the following, the standard color system *XYZ*, established by the International Lighting Commission CIE (*Commission Internationale de l'Eclairage*), will be described. This system represents the international reference system of color measurement.

3.1 STANDARD COLOR SYSTEM

The model of *additive color mixture* is used when light of differing wavelengths reaches an identical place on the retina or image sensor. The differing color stimuli are combined into one color through projective overlapping. Due to Grassmann's First Law of additive color mixture, any color stimulus can be uniquely related to a particular set of three primary color stimuli, as long as each primary stimulus is independent. By using vector notation, the unit length vectors of the primary colors can be viewed as a basis of a (not necessarily orthonormal) vector space.

Grassmann's First Law of color mixture can be written (applying vector addition) as

$$\mathbf{M} = R \cdot \mathbf{R} + G \cdot \mathbf{G} + B \cdot \mathbf{B}.$$

The quantities of primary colors **R, G, B** in the mixed color **M** are indicated by *R, G*, and *B*. However, not all colors can be produced with a single set of primary colors. This represents no injury to Grassmann's First Law of color mixture since the quantities of primary colors can be assumed to be negative in the color blending, for example:

$$\mathbf{M} + R \cdot \mathbf{R} = G \cdot \mathbf{G} + B \cdot \mathbf{B}.$$

The abovementioned principle of color blending is also valid for a set **M** of n colors. The following applies:

$$\mathbf{M} = \{\mathbf{M}_i | i = 1,\ldots,n\} \text{ with } \mathbf{M}_i = R_i \cdot \mathbf{R} + G_i \cdot \mathbf{G} + B_i \cdot \mathbf{B} \text{ and}$$

$$\mathbf{M}_{1\ldots n} = \mathbf{R} \cdot \sum_{i=1}^{n} R_i + \mathbf{G} \cdot \sum_{i=1}^{n} G_i + \mathbf{B} \cdot \sum_{i=1}^{n} B_i .$$

By an analysis of the visible wavelength interval in n narrow intervals, each interval approximately forms the color stimulus of a spectral color. Note that the waveband lies in general between 2 and 10 nm. A scanning that is too fine would result in a light density that is too low and not further measurable. If now the $\mathbf{M}_i$ from both of the abovenamed equations are color values of the spectral color intervals, any color stimulus can be described by additive mixture of a subset of $\boldsymbol{M}$ that corresponds to the spectral composition. If the waveband is shifted toward zero, then a continuous color stimulus $M(\lambda)$ in the form

$$M(\lambda) = R(\lambda) \cdot \mathbf{R} + G(\lambda) \cdot \mathbf{G} + B(\lambda) \cdot \mathbf{B}$$

is produced. For standardization, the International Lighting Commission (CIE) set the employed monochromatic primary values as well as the color matching functions in 1931 as the definition of the (hypothetical) colormetric *2° CIE standard observer*. Here 2° indicates the size of the visual field, which, until the introduction of the 10° CIE standard observer in 1964, should guarantee color perception without stimulation of the rods. The wavelengths and the relative spectral powers of the primary values are listed in Table 3.1. The color stimuli standardized with $S(\lambda)$ produce the *spectral tristimulus values* $\bar{r}(\lambda)$, $\bar{g}(\lambda)$ and $\bar{b}(\lambda)$. The following applies:

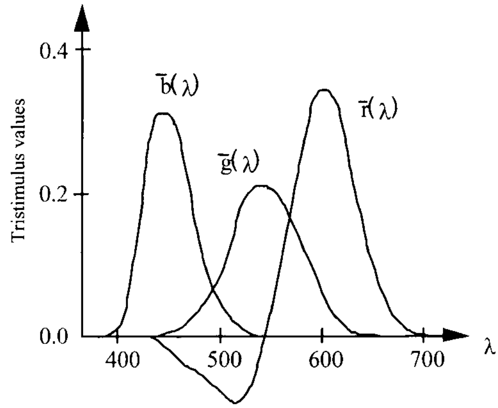

Figure 3.1. *The curves are representations of the CIE color matching functions* $\bar{r}, \bar{g}$, *and* $\bar{b}$ *for the 2° CIE standard observer.*

Primary	λ (in nm)	S
R	700.0	72.09
G	546.1	1.379
B	435.8	1.000

Table 3.1. *Wavelengths and the corresponding relative spectral power S of the CIE 1931 primaries.*

$$\overline{m}(\lambda) = \bar{r}(\lambda)\cdot\mathbf{R} + \bar{g}(\lambda)\cdot\mathbf{G} + \bar{b}(\lambda)\cdot\mathbf{B}\,.$$

The spectral values are dismantled in Fig. 3.1 as *color matching functions* over the visible wavelength area, whereby the units of the ordinates are arbitrarily fixed. See [TruKul96] concerning the problem of scanning the spectral value curves for certain uses in color image processing.

3.1.1 CIE Color Matching Functions

In order to obtain a color mixture that covers the entire visible wavelength area, the CIE defined virtual primary values *X*, *Y*, and *Z* (i.e., those that do not correspond to any physical spectral distribution). The conversion of the real spectral value curves into the positive, virtual color matching functions $\bar{x}(\lambda)$, $\bar{y}(\lambda)$ and $\bar{z}(\lambda)$ for the 2° CIE standard observer can be explained by the linear transformation

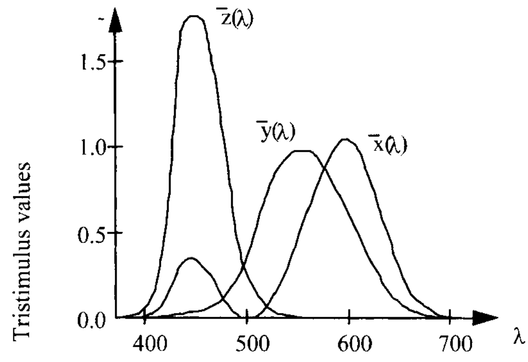

Figure 3.2. *The CIE color matching functions $\bar{x}, \bar{y}$, and $\bar{z}$ for the 2° CIE standard observer.*

$$\begin{pmatrix} \bar{x}(\lambda) \\ \bar{y}(\lambda) \\ \bar{z}(\lambda) \end{pmatrix} = \begin{pmatrix} 0.49000 & 0.31000 & 0.20000 \\ 0.17697 & 0.81240 & 0.01063 \\ 0.00000 & 0.01000 & 0.99000 \end{pmatrix} \cdot \begin{pmatrix} \bar{r}(\lambda) \\ \bar{g}(\lambda) \\ \bar{b}(\lambda) \end{pmatrix}.$$

The color matching functions that are assigned to the new spectral values can be taken from Fig. 3.2.

3.1.2 Standard Color Values

A radiation that causes a color stimulus in the eye is indicated as color stimulus function $\varphi(\lambda)$. For luminous objects, the color stimulus function is identical to the spectral power $S(\lambda)$. In comparison, in body colors, the color stimulus function is composed multiplicatively of the spectral power $S(\lambda)$ and the spectral reflection factor $R(\lambda)$. By observation of fluorescent samples, the fluorescence function $S_F(\lambda)$ is added for the color stimulus function of the body color. The following applies:

$$\varphi(\lambda) = \begin{cases} S(\lambda) & \text{for luminous objects} \\ S(\lambda) \cdot R(\lambda) & \text{for body colors} \\ S(\lambda) \cdot R(\lambda) + S_F(\lambda) & \text{for fluorescent samples} \end{cases}.$$

With that, the *standard color values* are determined by the equations

$$X = k \cdot \int \varphi(\lambda) \cdot \bar{x}(\lambda)\, d\lambda,$$
$$Y = k \cdot \int \varphi(\lambda) \cdot \bar{y}(\lambda)\, d\lambda \text{ , and}$$
$$Z = k \cdot \int \varphi(\lambda) \cdot \bar{z}(\lambda)\, d\lambda$$

with

$$k = \frac{100}{\int S(\lambda) \cdot \bar{y}(\lambda)\, d\lambda}.$$

The normalization factor k is used for body colors in order to achieve the value 100 for the standard color value $Y_{white\,body}$ for a pure pale, white body under illumination with any type of light. In practice the integral is changed into a sum on the basis of the finite measurements. For nonluminous objects, it should be taken into account that the color measurement depends on the measurement geometry. Therefore, a triple of the positive standard color values X, Y, and Z can be assigned to each spectral signal.

3.1.3 Chromaticity Diagrams

It is advantageous for a two-dimensional graphic representation to merely present an intersecting plane of the three-dimensional color space in a *chromaticity diagram*. Since all color values, whose position vectors are linearly dependent, differentiate themselves solely by brightness, simply the brightness information is lost. The color information that remains through elimination of brightness is indicated as *chromaticity*. In other words, chromaticity is defined by hue and saturation (without brightness). The commonly related intersection plane for the construction of the chromaticity diagram in the *RGB* cube is the unit plane $R + G + B = 1$, whereby an equilateral triangle results (see Fig. 3.3).

This triangle is also known as the *Maxwell color triangle*. M is the intersection between the observed color position vector and the unit plane. Using the Newtonian gravity formulation the following relationships result for a color M,

$$r_M = \frac{R}{R+G+B},\ g_M = \frac{G}{R+G+B}, \text{ and } b_M = \frac{B}{R+G+B}.$$

where $r_M + g_M + b_M = 1$. However, the Cartesian representation with r as abscissa and g as ordinate, by which blue lies in the origin, is more commonly used. The above relationships do not change by this. As an example of such a representation, the chromaticity diagram for the 2° CIE standard observer is shown in Fig. 3.4, in which two (of three) *2° chromaticity coordinates*, namely x and y, are represented. The position of the spectral colors from 400 - 700 nm is listed as *spectral color transmission*.

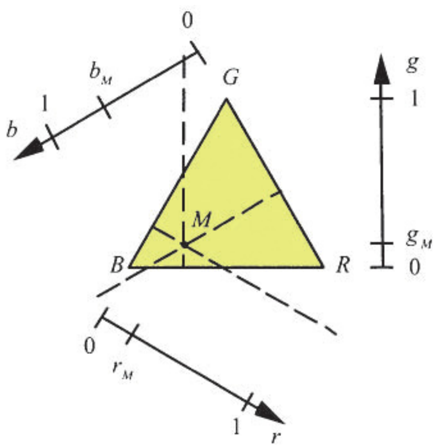

Figure 3.3. *Maxwell color triangle represented as a chromaticity diagram.*

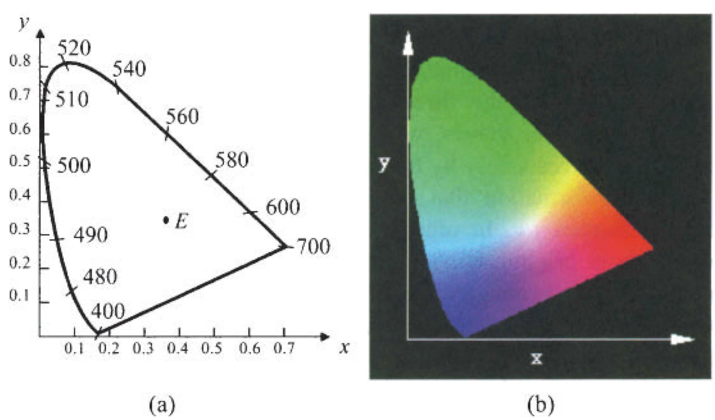

Figure 3.4. *The CIE chromaticity diagram of the 2° CIE standard observer (a) in numerical representation and (b) as color-coded illustration.*

The connection of the endpoints is called the *purple boundary*. All real chromaticities lie in the middle. The point that represents the equienergy spectrum $(x = y = z = 1/3)$, is indicated by *E*. The CIE chromaticity diagram can also be used for the definition of a *color gamut*, which shows the results of the addition of colors. By the addition of any two colors (e.g., *I* and *J* in Fig. 3.5) each color can be generated on its connecting line, in which the relative portions of both colors are varied. Through the use of a third color, *K*, a gamut with all the colors within the triangle *IJK* can be produced by mixing with *I* and *J*, in which again the relative portions are varied. On the basis of the form of the chromaticity diagram, it is obvious that not all colors can be produced through the mixture of the three colors red, green, and blue. No triangle can be constructed whose corners lie within the visible area and that covers the entire area.

The chromaticity diagram is also applied to compare color gamuts of different color monitors and different color printers [Fol et al. 94]. A comparison of different techniques for the reproduction of a device's color gamut in a color gamut of another device is explained in [MonFai97]. Since the color gamut of a color printer is relatively small in relation to the color gamut of a color monitor, not all colors can be printed on paper as seen on the monitor. A reduced gamut should be used for the monitor if the color images depicted on the screen are to be printed as true to the original as possible. Several image processing programs, like, for example, Adobe PhotoshopTM, support the user with a selection of a color gamut for the printing process.

3.1.4 MacAdam Ellipses

Since only brightness information is lost by the two-dimensional representation of colors, the chromaticity can be extracted from a chromaticity diagram by hue and saturation. A chromaticity can be described by specifying the wavelength of this spectral color and the ratio of the mixture. This is possible because the mixtures of two chromaticities of differing weighting lie on a line that connects these chromaticities. Also, according to Helmholtz, a color can be described as an additive mixture from a spectral color and an achromate (E) (with the exception of

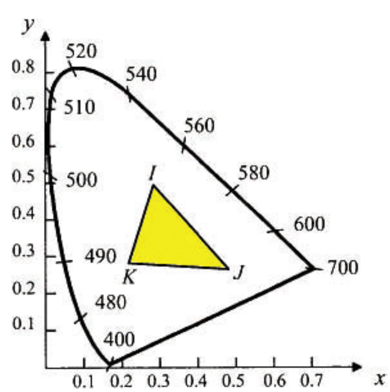

Figure 3.5. *By mixing the colors I and J, all colors can be produced on line IJ. By mixing the colors I, J, and K, all colors within the triangle IJK can be produced (after [Fol et al 94]).*

purple colors). These are the *dominant wavelength* λ_d , used for the description of hue, and the *excitation purity* p_e, for saturation.

The dominant wavelength of a chromaticity F can be constructed as point of intersection S of a ray arising in W and running through F with the spectral color transmission. With colors that do not have such a point of intersection, the purple boundary intersects them. The resulting wavelength is called the *complementary wavelength* λ_c. The spectral color component is defined as WF:WS.

Note that there exist differences of chromaticities, which are not perceived as equal, but are, however, equidistant in the chromaticity diagram. For example, more small color nuances can be differentiated in the green domain than in the blue domain. Examinations by MacAdam have revealed large discrepancies in the colors perceived as equal by the human visual system for differing reference color stimuli. From this, MacAdam obtained the distributions for 25 stimuli, which appear in the chromaticity diagram as ellipses (*MacAdam ellipses*) (see Fig. 3.6). The relationship of the area between the smallest and the largest ellipse amounts to approximately 0.94:69.4.

3.2 PHYSICS AND TECHNICS-BASED COLOR SPACES

Spaces that have a direct technical reference are presented below. As with the *RGB* color space, overlapping with physiological color spaces also occurs.

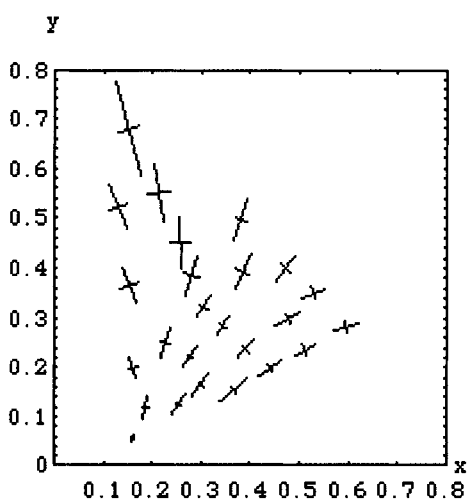

Figure 3.6. *In this chromaticity diagram for the 2° CIE standard observer, the MacAdam ellipses are represented by their two half-axes. The half-axes are scaled by a factor of 10. The data was adopted from [WysSti82] for this representation.*

3.2.1 *RGB* Color Spaces

The most commonly employed color space in computer technology is the *RGB color space*, which is based on the additive mixture of three primary colors **R**, **G**, and **B** (see Section 3.1). The international standardized wavelengths of the primary colors **R**ed, **G**reen, and **B**lue were already given in Table 3.1. It should be noted that the terms *red*, *green*, and *blue* were introduced solely for the purpose of standardization to provide descriptions for the primary colors. Visible colors and wavelengths are not equivalent. In order to avoid possible confusion, the notations *L*, *M*, *S* may be used for light containing long, middle, and short wavelengths instead of the notations *R*, *G*, *B*. However, the usual notations are *R*, *G*, and *B* and they will be used in the following.

The primary colors are for the most part the "reference colors" of the imaging sensors. They form the base vectors of a three-dimensional orthogonal (color)-vector space, where the zero-vector represents black (see Fig. 3.7). The origin is also described as *black point*. Any color can therefore be viewed as a linear combination of the base vectors in the *RGB* space. In one such accepted *RGB* color space, a color image is mathematically treated as a vector function with three components. The three vector components are determined by the measured intensities of visible light in the long-wave, middle-wave, and short-wave area. For a (three-channel) *digital color image* **C**, three vector components *R*, *G*, *B* are to be indicated for each image pixel (*x*,*y*):

$$\mathbf{C}(x,y) = \left(R(x,y), G(x,y), B(x,y)\right)^T = (R,G,B)^T.$$

These values are referred to as *tristimulus values*. The colors that are represented by explicit value combinations of the vector components *R*, *G*, *B*, are relative, device-dependent entities. All vectors $(R,G,B)^T$ with integer components $0 \le R,G,B \le G_{\max}$ characterize one color in the *RGB* color space. $G_{\max}+1$ indicates the largest permitted value in each vector component. Using permeable filters in the generation of a color image in the *RGB* color space, so-called red, green, and blue extracts are generated in the long wave, middle wave and short wave area of visible light. If one refrains from using the filter, each of the three scannings is identical with the digitalization of a gray-level image. The rational numbers

$$r = \frac{R}{R+G+B}, \quad g = \frac{G}{R+G+B}, \text{ and } b = \frac{B}{R+G+B} \tag{3.1}$$

are the color value components that are normalized with respect to the intensity (see Section 3.1.3).

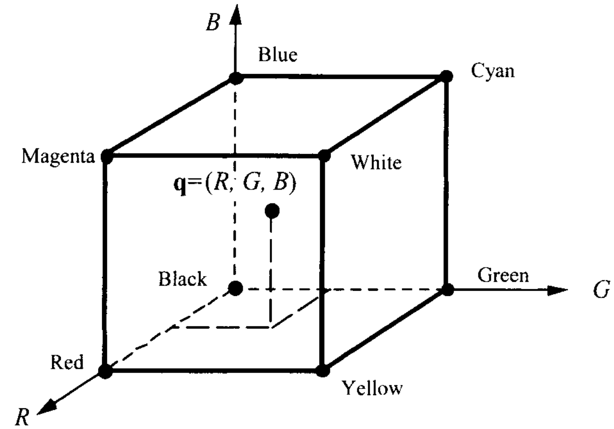

Figure 3.7. *In the RGB color space, every vector* $\mathbf{q} = (R,G,B)^T$ *inside the color cube represents exactly one color, where* $0 \le R,G,B \le G_{\max}$ *and R, G, B are integers.*

The primary colors red $(G_{\max},0,0)^T$, green $(0,G_{\max},0)^T$, blue $(0,0,G_{\max})^T$, and the complementary colors yellow $(G_{\max},G_{\max},0)^T$, magenta $(G_{\max},0,G_{\max})^T$, cyan $(0,G_{\max},G_{\max})^T$, as well as the achromatic colors white $(G_{\max},G_{\max},G_{\max})^T$ and black $(0,0,0)^T$, represent the boundaries of the color cube, which is formed through the possible value combinations of R, G, B. All color vectors $(R,G,B)^T$ with $0 \le R,G,B \le G_{\max}$ each characterize a color in the *RGB* color space. This color cube is represented in Fig. 3.7. All achromatic colors (gray tones) lie on the principal diagonal $(u,u,u)^T$, with $0 \le u \le G_{\max}$.

The *RGB* color space is the most applied computer-internal representation of color images. Its wide distribution is, among other things, traced back to the well-standardized three primary colors. Almost all visible colors can be represented by a linear combination of the three vectors (see Section 3.1.3). For identical objects, differing color values are generated with different cameras or scanners since their primary colors in general do not match. The process of adjusting color values between different devices (e.g., camera*RGB*, monitor*RGB*, and printer*RGB*) is called *color management*. See [Har01] and [GioMad98] for an introduction to color management.

A special case of the *RGB* color space is the primary color system $R_N G_N B_N$ for television receivers (*receiver primary color system*), which refers to the established phosphors in the American standard NTSC (National Television System Committee). Values deviating from this are valid for the phosphors through the television standards PAL (Phase Alternation Line) and SECAM (Séquentiel Couleur à Mémoire). The *RGB* color space, which was determined by the CIE, is transformed [Pra91] into the NTSC-primary color system $R_N G_N B_N$ through

$$\begin{pmatrix} R_N \\ G_N \\ B_N \end{pmatrix} = \begin{pmatrix} 0.842 & 0.156 & 0.091 \\ -0.129 & 1.320 & -0.203 \\ 0.008 & -0.069 & 0.897 \end{pmatrix} \cdot \begin{pmatrix} R \\ G \\ B \end{pmatrix} \tag{3.2}$$

In 1996, the International Color Consortium (ICC) proposed a standard color space *sRGB* for the Internet [Sto et al. 96]. The standard considers cathode ray tube (CRT) monitors and D_{65} daylight. The reference viewing environment parameters can be found in [Sto et al. 96]. *sRGB* tristimulus values are simply linear combinations of the CIE *XYZ* values. They are also known as Rec. 709 *RGB* values and they can be computed using the following relationship:

$$\begin{pmatrix} R_{sRGB} \\ G_{sRGB} \\ B_{sRGB} \end{pmatrix} = \begin{pmatrix} 3.2410 & -1.5374 & -0.4986 \\ -0.9692 & 1.8760 & 0.0416 \\ 0.05556 & -0.2040 & 1.0570 \end{pmatrix} \cdot \begin{pmatrix} X \\ Y \\ Z \end{pmatrix} \tag{3.3}$$

In a second processing step (which modifies the value of the gamma correction factor used in the ITU-R BT.709 standard), these values are transformed to nonlinear s*R'G'B'* values as follows:

If $R_{sRGB}, G_{sRGB}, B_{sRGB} \leq 0.0034$ **then**

$$sR' = 12.92 R_{sRGB}$$
$$sG' = 12.92 G_{sRGB}$$
$$sB' = 12.92 B_{sRGB}$$

else if $R_{sRGB}, G_{sRGB}, B_{sRGB} > 0.0034$ **then**

$$sR' = 1.055 R_{sRGB}{}^{1.0/2.4} - 0.055$$
$$sG' = 1.055 G_{sRGB}{}^{1.0/2.4} - 0.055\,.$$
$$sB' = 1.055 B_{sRGB}{}^{1.0/2.4} - 0.055$$

end {if}

The effect of the above equations is to closely fit a straightforward gamma 2.2 curve with a slight offset to allow for invertability in integer math [Sto et al. 96]. Finally, the nonlinear *sR'G'B'* values are converted to digital code values by

$$
\begin{aligned}
R &= G_{\max} \cdot sR' \\
G &= G_{\max} \cdot sG' \quad . \\
B &= G_{\max} \cdot sB'
\end{aligned}
$$

This transformation proposes using a black digital count of 0 and a white digital count of 255 for 24-bit (8-bits/channel) encoding (which is different from digital broadcast television using a black digital count of 16 and a white digital count of 235 in order to provide a larger encoded color gamut).

Note that the Internet standard *sRGB* is made for CRT monitors under daylight viewing conditions. However, many people work under nondaylight conditions and/or they use notebooks with liquid crystal displays (LCDs). Recently, several modifications of the *sRGB* are proposed for extended color gamuts (e.g., e-sRGB, scRGB, ROMM RGB, RIMM RGB). For an overview on *RGB* color spaces see, for example, [Süs et al. 99] and [Spa et al. 00].

3.2.2 *CMY(K)* Color Space

In the printout of a color image with a color printer, the *CMY(K)* color space, with the subtractive primary colors cyan, magenta, and yellow as well as possibly an additional black (*K*arbon), is used. A subtractive color space forms the basis for the printing process. Since cyan, magenta, and yellow are the complementary colors to red, green, and blue, the *RGB* color space and the *CMY* color space can be transferred through

$$
\begin{pmatrix} R \\ G \\ B \end{pmatrix} = \begin{pmatrix} G_{\max} \\ G_{\max} \\ G_{\max} \end{pmatrix} - \begin{pmatrix} C \\ M \\ Y \end{pmatrix} \quad \text{and} \quad \begin{pmatrix} C \\ M \\ Y \end{pmatrix} = \begin{pmatrix} G_{\max} \\ G_{\max} \\ G_{\max} \end{pmatrix} - \begin{pmatrix} R \\ G \\ B \end{pmatrix} \tag{3.4}
$$

into one another, where $G_{\max} + 1$ again denotes the greatest representable value in each color channel. As in the *RGB* color space, a color cube represents the *CMY* color space (see Fig. 3.8).

Frequently, additional black ink is used in printing. There are essentially three reasons for this: First, the printing, one on top of the other, of the colors cyan, magenta, and yellow leads to a larger emission of fluid and with that come longer drying times. Second, it can occur, on the basis of mechanical tolerances, that the three color inks do not print exactly on the same position. Because of this, colored edges develop along black borders. Third, the black ink is less expensive to manufacture than the three color inks. Toward the end of the *CMY* color space, black is used in place of the same portions of *C*, *M*, and *Y* in accordance with the relations

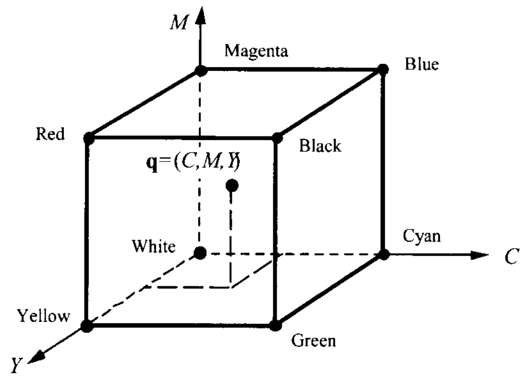

Figure 3.8. *The CMY color space for color printing.*

$$K = min(C, M, Y),$$
$$C = C - K,$$
$$M = M - K, \text{ and}$$
$$Y = Y - K.$$

In the *CMY* color space it is assumed that filters with nonoverlapping spectral absorption curves exist for the three subtractive primary colors. In practice, the dyes and printer inks used in the printing technology frequently have absorption curves that severely overlap. Through this, nonlinear dependencies between the printing colors develop in the color mixture. In addition, the printed result is influenced by the various representations of the printed color depending on the number of ink dots per inch and the composition of the paper as well as the material to be printed [Poy97]. These complex correlations will not be covered further at this point.

3.2.3 *YIQ* Color Space

In the development of the NTSC television system used in the United States, a color coordinate system with the coordinates *Y*, *I*, and *Q* was defined for transmission purposes. To transmit a color signal efficiently, the $R_N G_N B_N$ signal was more conveniently coded from a linear transformation. The luminance signal is coded in the *Y*-component. The additional portions *I* (*in-phase*) and *Q* (*quadrature*) contain the entire chromaticity information that is also denoted as *chrominance signal* in television technology.

I and *Q* are transmitted by a much shorter waveband since the *Y* signal contains by far the largest part of the information. The *Y* signal contains no color information so that the *YIQ* system remains compatible with the black-white system. By using only the Y signal in a black-and-white television, gray-level images can be displayed, which would not be possible by a direct transmission of the $R_N G_N B_N$ signal.

The values in the $R_N G_N B_N$ color space can be transformed with

$$\begin{pmatrix} Y \\ I \\ Q \end{pmatrix} = \begin{pmatrix} 0.299 & 0.587 & 0.114 \\ 0.596 & -0.274 & -0.322 \\ 0.211 & -0.523 & 0.312 \end{pmatrix} \cdot \begin{pmatrix} R_N \\ G_N \\ B_N \end{pmatrix} \tag{3.5}$$

into the values in the YIQ color space.

3.2.4 *YUV* Color Space

The color television systems PAL and SECAM, developed in Germany and France, use the YUV color space for transmission. The Y component is identical with the one of the YIQ color space. The values in the $R_N G_N B_N$ color space can be transformed with

$$\begin{pmatrix} Y \\ U \\ V \end{pmatrix} = \begin{pmatrix} 0.299 & 0.587 & 0.114 \\ -0.418 & -0.289 & 0.437 \\ 0.615 & -0.515 & -0.100 \end{pmatrix} \cdot \begin{pmatrix} R_N \\ G_N \\ B_N \end{pmatrix} \tag{3.6}$$

into the values in the YUV color space [Pra91]. On account of the low information content, the U and V signals, which are usually related to the Y signal, are reduced by half (two successive image pixels each having a separate Y portion, but with a common color type) and by a quarter for simple demands.

The I and Q signals of the YIQ color space are determined from the U and V signals of the YUV color space by a simple rotation in the color coordinate system. The following applies [Pra91]:

$$I = -U \cdot \sin(33°) + V \cdot \cos(33°),$$

$$Q = U \cdot \cos(33°) + V \cdot \sin(33°).$$

Presentations in the YIQ and YUV color space are very suitable for image compression since luminance and chrominance can be coded with different numbers of bits, which is not possible when using RGB values.

In the literature, YUV also indicates a color space, in which U corresponds to the color difference red-blue and V to the color difference green-magenta. Y corresponds to the equally weighted (arithmetical) averages of red, green, and blue. This color space is, for example, employed in highlight analysis of color images (see Section 8.1.4). We will denote this color space with $(YUV)'$ for a better distinction. A linear correlation exists between the $(YUV)'$ color space and the RGB system, which is given by the transformation

$$(Y,U,V)' = (R,G,B)\begin{pmatrix} \frac{1}{3} & \frac{1}{2} & \frac{-1}{2\sqrt{3}} \\ \frac{1}{3} & 0 & \frac{1}{\sqrt{3}} \\ \frac{1}{3} & \frac{-1}{2} & \frac{-1}{2\sqrt{3}} \end{pmatrix}. \tag{3.7}$$

Brightness normalization can be defined by

$$u = \frac{U}{R+G+B} \quad \text{and} \quad v = \frac{V}{R+G+B}. \tag{3.8}$$

If u and v form the axes of a Cartesian coordinate system, then red, green, and blue stretch an equilateral triangle in which black lies in the origin (see Fig. 3.9).

3.2.5 YC_BC_R Color Space

In the area of digital video, which is increasingly gaining importance, the internationally standardized YC_BC_R color space is employed for the representation of color vectors. This color space differs from the color space used in analog video recording, which will not be gone into at this point. A detailed description of digital and analog video technology is included in [Poy96]. The values in the $R_NG_NB_N$ color space can be transformed into the values in the YC_BC_R color space [Poy96]:

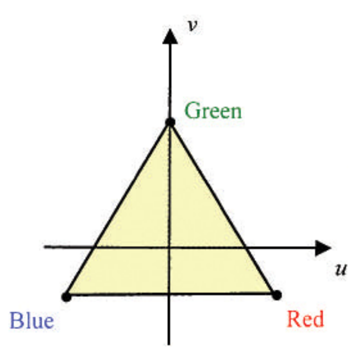

Figure 3.9. *The uv-plane of the $(YUV)'$-model.*

$$\begin{pmatrix} Y \\ C_B \\ C_R \end{pmatrix} = \begin{pmatrix} 16 \\ 128 \\ 128 \end{pmatrix} + \frac{1}{256} \begin{pmatrix} 65.738 & 129.057 & 25.064 \\ -37.945 & -74.494 & 112.439 \\ 112.439 & -94.154 & -18.285 \end{pmatrix} \cdot \begin{pmatrix} R_N \\ G_N \\ B_N \end{pmatrix}$$

From this transformation it is assumed that the *RGB* data has already undergone a gamma correction. The quantities for the *Y* components refer to the fixed values for phosphors in the reference Rec. ITU-R BT.601-4 of the NTSC system. The back transformation from the YC_BC_R color space into the $R_NG_NB_N$ color space is (except for a few rounding errors) given by

$$\begin{pmatrix} R_N \\ G_N \\ B_N \end{pmatrix} = \frac{1}{256} \begin{pmatrix} 298.082 & 0.0 & 408.583 \\ 298.082 & -100.291 & -208.120 \\ 298.082 & 516.411 & 0.0 \end{pmatrix} \cdot \begin{pmatrix} Y-16 \\ C_B-128 \\ C_R-128 \end{pmatrix}$$

[Poy96]. The YC_BC_R color space was developed for representations in the television format common until now. It does not apply to the HDTV (*high definition television*) format.

3.2.6 Kodak PhotoCD YC_1C_2 Color Space

The Kodak Company developed the YC_1C_2 color space for their PhotoCD system. The YC_1C_2 color space is quite similar to the YC_BC_R color space. The differences are that the color gamut of the YC_1C_2 color space was adapted as closely as possible to the color gamut of photographic film, while the color gamut of the YC_BC_R color space orientates itself to the phosphors of the NTSC system. The values in the $R_NG_NB_N$ color space can be obtained from the PhotoCD YC_1C_2 color space with the equation

$$\begin{pmatrix} R_N \\ G_N \\ B_N \end{pmatrix} = 255 \cdot \begin{pmatrix} 0.00549804 & 0.0 & 0.0051681 \\ 0.00549804 & -0.0015446 & -0.0026325 \\ 0.00549804 & 0.0079533 & 0.0 \end{pmatrix} \cdot \begin{pmatrix} Y \\ C_1-156 \\ C_2-137 \end{pmatrix}$$

[Poy96]. It should be taken into consideration that on the PhotoCD, the C_1 and C_2 components are subsampled both horizontally and vertically by a factor of 2 for compression purposes. This is, however, an integral part of the PhotoCD system's compression and not an element of the YC_1C_2 color space.

3.2.7 $I_1I_2I_3$ Color Space

The $I_1I_2I_3$ color space depicts a feature model rather than a color space. In an examination of eight randomly chosen color images and eleven color spaces, Ohta, Kanade, and Sakai [Oht et al. 80] achieved the best segmenting results in color images by using the $I_1I_2I_3$ color space. Due to these good results this color space is frequently used in color image processing. The three components are defined by

$$I_1 = \frac{R+G+B}{3},\ I_2 = \frac{R-B}{2}\ \text{, and } I_3 = \frac{2G-R-B}{4}. \tag{3.9}$$

Note the similarity between the $I_1I_2I_3$ color space and the opponent color space.

3.3 UNIFORM COLOR SPACES

A *uniform color space* is a color space in which same-size changes in the color coordinates also correspond to same-size recognizable changes in the visible color tones and color saturation. This is not the case with physically and technically oriented color spaces, which were described in the previous section. In order to reduce such variations, several revised color spaces were defined. However, no color space exists that allows an undistorted or unbiased representation. Therefore, "uniform" means in this sense "more or less uniform." The international lighting commission CIE recommended the $L^*a^*b^*$ *color space CIE 1976* and the $L^*u^*v^*$ *color space CIE 1976* as an approximation of uniform color spaces. The German institute of standardization DIN (Deutsches Institut für Normierung) also adopted these color spaces. These are usually abbreviated as CIELAB and CIELUV.

Both color spaces are derived from the *XYZ* standard color system (*CIE XYZ primary system*). The calibration of the measured camera data in the *XYZ* standard color space presents a complex problem, which is the subject of Section 4.5.4. In the following section, the CIELAB color space and the CIELUV color space are described. Uniform color spaces are interesting for several areas of color image processing applications, especially if very similar colors have to be compared. Both these color spaces are device-independent color spaces. However, they are computationally intensive to transform to other color spaces. This is a drawback if video real-time processing is required, that is 24 frames per second.

3.3.1 CIELAB Color Space

The CIELAB color space was developed in order to obtain an easy-to-calculate color measurement that is in accord with the Munsell color order system (see Section 3.6.1). The following conversion is valid for $X/X_n, Y/Y_n, Z/Z_n >$

0.008856. It is further expanded for X/X_n, Y/Y_n, $Z/Z_n \leq 0.008856$ (see CIE, DIN 5033, and DIN 6174). The following applies:

$$\begin{aligned} X^* &= \sqrt[3]{X/X_n} && \text{for } X/X_n > 0.008856 \\ X^* &= 7.787 \cdot (X/X_n) + 0.138 && \text{for } X/X_n \leq 0.008856 \end{aligned} \tag{3.10a}$$

$$\begin{aligned} Y^* &= \sqrt[3]{Y/Y_n} && \text{for } Y/Y_n > 0.008856 \\ Y^* &= 7.787 \cdot (Y/Y_n) + 0.138 && \text{for } Y/Y_n \leq 0.008856 \end{aligned} \tag{3.10b}$$

$$\begin{aligned} Z^* &= \sqrt[3]{Z/Z_n} && \text{for } Z/Z_n > 0.008856 \\ Z^* &= 7.787 \cdot (Z/Z_n) + 0.138 && \text{for } Z/Z_n \leq 0.008856 \end{aligned} \tag{3.10c}$$

$$\begin{aligned} L^* &= 116 \cdot Y^* - 16, \\ a^* &= 500 \cdot (X^* - Y^*), \\ b^* &= 200 \cdot (Y^* - Z^*). \end{aligned} \tag{3.11}$$

On this occasion (X_n, Y_n, Z_n) describes the white reference point, which represents a perfectly matte white body under an illuminant (e.g., *D*65, *A* or *C*; see Section 4.2.2). *X*, *Y*, and *Z* are the values in the standard color system (see Section 3.1.2). L^* is also indicated as L^*-*lightness* (pronounced *L-star-lightness*) and is scaled approximately equidistant according to sensitivity. The functional relations between *Y* and L^* are represented for $Y_n = 100$ in Fig. 3.10.

It should be understood that equally distant differences between *Y* pairs are more strongly noticeable in the dark area than in the lighter area. In contrast to the

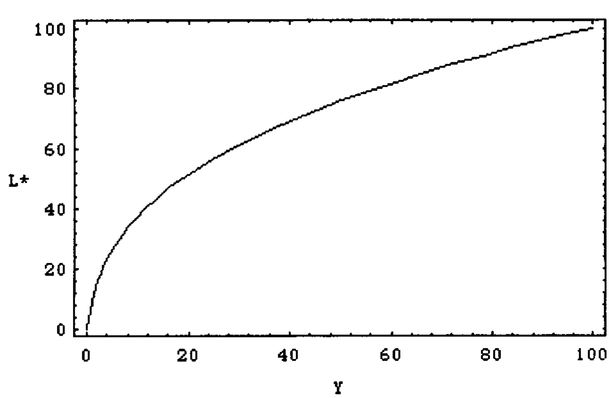

Figure 3.10. L^*-*lightness for* $Y_n = 100$.

standard CIE chromaticity diagram and the (u',v') chromaticity diagram, chromaticities cannot be clearly assigned to the chromaticity points, the (a^*, b^*) chromaticity diagrams, which belong to the CIELAB color space since their position depends on L^*. By constant L^*, chromaticity points that lie on a straight line in the standard color table become curved.

For the improvement of the uniformity of the color appearance, modifications to the CIELAB color space were continually developed. A recent example of this is called the LLAB color space, the description of which is referred to in [Luo96]. Furthermore, several approximations of the CIELAB color space were suggested in order to accelerate the computationally intensive conversion of data in the *RGB* color space into the CIELAB color space [ConFli97]. Especially mathematically efficient is the single calculation of a number of $L^*a^*b^*$ values and their storage in a lookup table. If all $L^*a^*b^*$ values for all possible *RGB* values were stored, then the lookup table, with a quantization of eight bits, would have to contain about 16 million entries. However, the number of entries in the table can be considerably reduced by an approximation of the $L^*a^*b^*$ values. The maximum error between the correct values and the approximate values that arises from this can be determined from Eq. (3.17) described later in Section 3.5.3. In a lookup table with 2000 real-valued entries, the error amounts to $\Delta E^*_{ab} = 1.96$ units, and with 8000 entries, it decreases to $\Delta E^*_{ab} = 0.6$ units. The CIELAB color space (see Fig. 3.11) is used for the description of body colors (for nonluminous materials), whereas the CIELUV color space described in the following (see Fig. 3.12) is usually used for the description of colors of light.

3.3.2 CIELUV Color Space

The chromaticity diagram of the CIELUV color space is indicated as the *CIE 1976 uniform chromaticity scale diagram* (or *CIE 1976 UCS diagram*). In accordance with DIN 5033, the term (u',v')-space is also used. The CIELUV color space is defined using the symbols taken from the previous section:

$$\begin{aligned} L^* &= 116 \cdot \sqrt[3]{Y/Y_n} - 16 \quad && \text{for } Y/Y_n > 0.008856 \\ X^* &= 903.3 \cdot (Y/Y_n) && \text{for } Y/Y_n \leq 0.008856 \end{aligned} \tag{3.12a}$$

$$\begin{aligned} u^* &= 13 \cdot L^* \cdot (u' - u'_n)\,, \\ v^* &= 13 \cdot L^* \cdot (v' - v'_n) \end{aligned} \tag{3.12b}$$

with

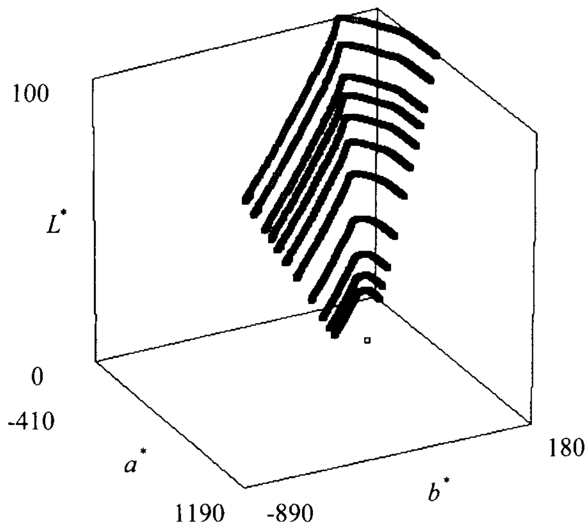

Figure 3.11. *Illustration of the 2° spectral color transmission for Y = 0, 2, 3, 5, 10, 20, 30, 40, 50, 60, 80, and 100 in the CIELAB color space. A point results for Y = 0 (black). Illuminant C is used as white reference.*

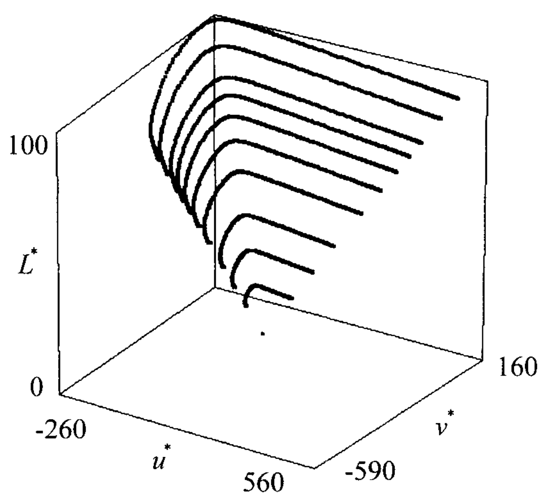

Figure 3.12. *Depiction of the 2° spectral color transmission for Y = 0, 2, 3, 5, 10, 20, 30, 40, 50, 60, 80 and 100 in the CIELUV color space. For Y = 0 (black) a point is shown. As white reference the standard illuminant C was assumed.*

$$u' = \frac{4 \cdot X}{X + 15 \cdot Y + 3 \cdot Z} = \frac{4 \cdot x}{3 - 2 \cdot x + 12 \cdot y},$$

$$u'_n = \frac{4 \cdot X_n}{X_n + 15 \cdot Y_n + 3 \cdot Z_n} = \frac{4 \cdot x_n}{3 - 2 \cdot x_n + 12 \cdot y_n},$$

and

$$v' = \frac{9 \cdot Y}{X + 15 \cdot Y + 3 \cdot Z} = \frac{9 \cdot y}{3 - 2 \cdot x + 12 \cdot y},$$

$$v'_n = \frac{9 \cdot Y_n}{X_n + 15 \cdot Y_n + 3 \cdot Z_n} = \frac{9 \cdot y_n}{3 - 2 \cdot x_n + 12 \cdot y_n}.$$

The L^*-component is identical to the L^*-component in the CIELAB color space. In contrast to the CIELAB color space, straight lines are again mapped onto straight lines in the CIELUV color space, which is a great advantage to additive mixture calculations.

The sizes of wavelengths with the same hue and the sizes that correspond to the spectral color proportion are indicated as *hue angles* h^*_{ab}, h^*_{uv} and *chroma* C^*_{ab}, C^*_{uv}. The following applies:

$$h^*_{ab} = \arctan(b^* / a^*), \qquad h^*_{uv} = \arctan(v^* / u^*),$$
$$C^*_{ab} = \sqrt{a^* \cdot a^* + b^* \cdot b^*}, \quad C^*_{uv} = \sqrt{u^* \cdot u^* + v^* \cdot v^*}. \tag{3.13}$$

For the CIELUV color space the relation of multicoloredness to brightness is defined as a measure of saturation by

$$S^*_{uv} = C^*_{uv} / L^* = 13\sqrt{(u' - u'_n) \cdot (u' - u'_n) + (v' - v'_n) \cdot (v' - v'_n)}\,. \tag{3.14}$$

3.4 PERCEPTION-BASED COLOR SPACES

Color spaces that are based intuitively on human color perception are of interest for the fields of computer vision and computer graphics. With the *HSI* and the *HSV* color spaces, the wish for user-friendly input and description of color values is in the foreground. A color can be more easily described intuitively (above all by untrained users) by values for hue, color saturation, and intensity than from vector components in the *RGB* or *CMYK* color space.

3.4.1 *HSI* Color Space

In the *HSI* color space *hue*, *saturation*, and *intensity* are used as coordinate axes. Fig. 3.13 shows a possible representation of the *HSI* color space. This color space is well suited for the processing of color images and for visually defining interpretable local characteristics. A color $\mathbf{q} = (R, G, B)^T$ is given in the *RGB* color space. The hue H of the color $\mathbf{q}$ characterizes the dominant color contained in $\mathbf{q}$. Red is specified as a "reference color." Because of that, $H = 0°$ and $H = 360°$ correspond to the color red. Formally, H is given by

$$H = \begin{cases} \delta & \text{if } B \le G \\ 360° - \delta & \text{if } B > G \end{cases} \tag{3.15a}$$

with

$$\delta = \arccos\left(\frac{(R-G)+(R-B)}{2\sqrt{(R-G)^2 + (R-B)\cdot(G-B}} \right).$$

The saturation S of the color $\mathbf{q}$ is a measurement of color purity. This parameter is dependent on the number of wavelengths that contribute to the color perception. The wider the range of the wavelengths, the lower the purity of the color. The more narrow the range of the wavelengths, the higher the purity of the color. The extreme case $S = 1$ is true for a pure color and the extreme case $S = 0$ for an achromatic color. S is given by

$$S = 1 - 3 \cdot \frac{\min\,(R, G, B)}{R+G+B}. \tag{3.15b}$$

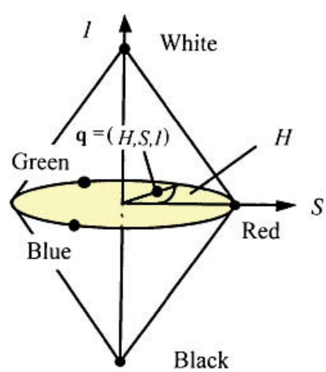

Figure 3.13. *The HSI-color space.*

The *intensity* I of the color $\mathbf{q}$ corresponds to the relative brightness (in the sense of a gray-level image). The extreme case $I = 0$ corresponds to the color black. The intensity is defined in accordance with

$$I = \frac{R+G+B}{3}. \tag{3.15c}$$

For the color $\mathbf{q} = (R, G, B)^T$ in the *RGB* color space, a representation $(H, S, I)^T$ of this color is given in the *HSI* color space. This conversion is clearly reversible (except for inaccuracies in rounding and some singularities). The back transformation is given in Fig. 3.14.

```
if (S = 0) then                                        {gray tone}
    R = G = B = I ;
else
    if (0 ≤ H ≤ 120) then                              {B is minimum}
        B = (1 − S) · I ;
        H = (1/√3) · tan(H − 60) ;
        G = (1.5 + 1.5 · H) · I − (0.5 + 1.5 · H) · B ;
        R = 3 · I − G − B
    else
        if (120 ≤ H ≤ 240) then                        {R is minimum}
            R = (1 − S) · I ;
            H = (1/√3) · tan(H − 180) ;
            B = (1.5 + 1.5 · H) · I − (0.5 + 1.5 · H) · R ;
            G = 3 · I − B − R
        else                                           {G ist minimum}
            G = (1 − S) · I ;
            H = (1/√3) · tan(H − 300) ;
            R = (1.5 + 1.5 · H) · I − (0.5 + 1.5 · H) · G ;
            B = 3 · I − R − G
        end {if}
    end {if}
end {if}
```

Figure 3.14. *Conversion of color images from the HSI representation into a RGB representation (according to [Fre88]).*

One of the advantages of the *HSI* color space is the separation of chromatic and achromatic information. The existence of singularities is a disadvantage for the *HSI* color space. Furthermore, it must be observed that the information content and the reliability of the calculation of hue and saturation depend on the luminosity (see [Fre88] and [Fre90]). In achromatic colors, neither hue nor saturation is defined. The characteristic nonlinearity of the cameras in general can affect the *HSI* conversion unfavorably (see Section 4.4.1).

Transformations between the color spaces can be significantly accelerated when using hardware. Image processing boards are available for PCs and workstations that transfer a video image (in NTSC or PAL format) or an *RGB* image into an *HSI* image in real time. The back transformation of *HSI* into the *RGB* color space can be derived from Eq. (3.15abc). The algorithm is given in pseudocode in Fig. 3.14.

3.4.2 *HSV* Color Space

The *HSV* color space, which is also called the *HSB* color space, is particularly common in the field of computer graphics. As in the *HSI* color space, hue, saturation, and brightness value are used as coordinate axes. By projecting the *RGB* unit cube along the diagonals of white to black, a hexacone results that forms the topside of the *HSV* pyramid. The hue *H* is indicated as an angle around the vertical axle. As in the *HSI* color space, red is determined with $H = 0°$ or $H = 360°$, green with $H = 120°$, and so on (see Fig. 3.15).

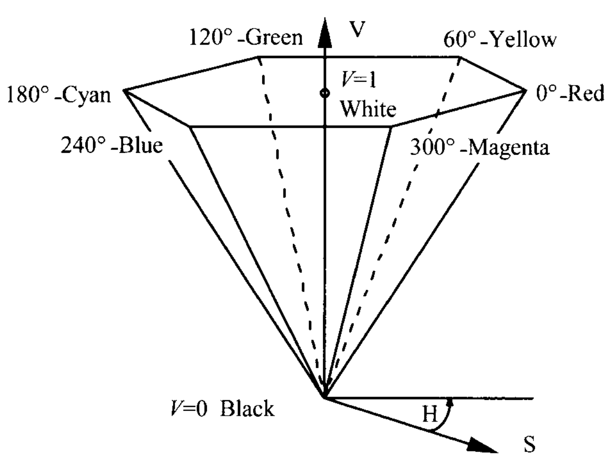

Figure 3.15. *Hexacone representation of the HSV color space.*

The saturation S is a number between 0 on the central axis (the V-axis) and 1 on the sides of the pyramid. For $S = 0$, H is undefined. The brightness value V (or B) lies between 0 on the apex of the pyramid and 1 on the base. The point on the apex of the pyramid with $V = 0$ is black. At this point, the values of H and S have no significance. The lightest colors lie on the topside of the pyramid; however, not all colors with the same brightness are visible on the plane $V = 1$. The pseudocode for the conversion of a color image from the RGB color space into the HSV color space is indicated in Fig. 3.16, where again $G_{max} + 1$ denotes the largest possible value in each color channel. A representation of the back transformation is not given here but can be found in [Fol et al. 94]. Some image processing programs (e.g., Adobe PhotoshopTM) contain modules for transforming images between the RGB and the HSV representation (there called HSB).

```
max = Max(R,G,B);
min = Min(R,G,B);
V = max / Gmax ;                                            {brightness value}
if (max ≠ 0) then S = (max − min) / max                     {saturation value}
              else S = 0 ;
                   H = UNDEFINED
end {if};
if (S > 0) then
    DR = (max − R) /(max − min);
    DG = (max − G) /(max − min);
    DB = (max − B) /(max − min);
    if (max = R) then if (min = G) then H = 5 + DB            {color between
                      else H = 1 − DG                     magenta and yellow}
    else if (max = G) then if (min = B) then H = 1 + DR       {color between
                           else H = 3 − DB                   yellow and cyan}
    else if (min = R) then H = 3 + DG                         {color between
                      else H = 5 − DR ;                             cyan and
    end {if}                                                        magenta}
    if (H < 6) then H = H · 60
                else H = 0 ;
end {if}
```

Figure 3.16. *Conversion of color images from the RGB representation into an HSV representation.*

With both the *HSV* and the *HSI* color spaces described in the previous paragraph, there exists the problem, apart from the singularities in the color space already specified, that a straight line in the *RGB* space is not generally mapped onto a straight line in the two other color models. Here in particular it is to be noted in the cases of interpolations in the color spaces and transformations between the color spaces. An advantage of the *HSV* color space lies in the fact that it intuitively corresponds to the color system of a painter when mixing the colors and its operation is very easy to learn. In digital color image processing, the *HSV* color space is of only secondary importance. It is used for the easily operated manipulation of a color image's color values (e.g., with Adobe PhotoshopTM).

3.4.3 Opponent Color Spaces

In the opponent color theory or four-color theory, antagonistic neural processes, with the opponent colors red-green and blue-yellow and likewise an antagonistically organized light-dark system, are named as the basis for human color vision (see Section 2.3). Fig. 3.17 shows one presentation of the opponent color space. The receptive field of an opponent color cell is divided into a center system and a peripheral system (see Section 2.3). In color image processing, both systems are also modeled by two-dimensional, rotationally symmetrical Gaussian functions. The opponent color space is used, for example, in color stereo analysis [BroYan89] (see Chapter 9), in color image segmentation [Hol82] (see Chapter 7), and in an approximation of color constancy (see Chapter 8).

3.5 COLOR DIFFERENCE FORMULAS

In virtually all areas of color image processing it is necessary to compare colors within an image or between several images. The difference between two colors in a color space must be determined and described. In the following, some measurements of color difference are given as examples for the *RGB* color space, the *HSI* color space, the CIELAB color space, and the CIELUV color space.

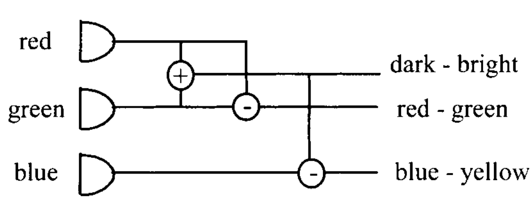

Figure 3.17. *A representation of the opponent color space (after [BroYan89]).*

3.5.1 Color Difference Formulas in the *RGB* Color Space

If the *RGB* space is regarded as Euclidean space, then known distance measurements can be adopted for the calculation of a color difference. A metric (e.g., the Euclidean metric) is to be selected. The color distance can be used in accordance with Eq. (3.1) for the color value quantities, standardized by intensity, as well as for the nonstandardized values. The color distance measurement can be used both for the color proportional values $(r,g,b)^T$ standardized in accordance with Eq. (3.1) by intensity, and for the nonstandardized values. In the *RGB* color space, the Euclidean distance between two color vectors $\mathbf{F}_1$ and $\mathbf{F}_2$ represents the angle between the two vectors (see Fig. 3.18). These distance measurements are widely used within the area of color image processing on account of their simple predictability. However, there is no connection between these distance measurements and human color perception.

3.5.2 Color Difference Formulas in the *HSI* Color Space

The formulas valid in the *RGB* color space are not suitable for a difference measurement in the *HSI* color space. For example, the color difference Δ_{HSI} can be used there [TseCha92]. For two color values $\mathbf{F}_1 = (H_1, S_1, I_1)^T$ and $\mathbf{F}_2 = (H_2, S_2, I_2)^T$ in the *HSI* color space, the color difference between them is determined by

$$\Delta_{HSI}(\mathbf{F}_1, \mathbf{F}_2) = \sqrt{(\Delta_I)^2 + (\Delta_C)^2} \tag{3.16}$$

with

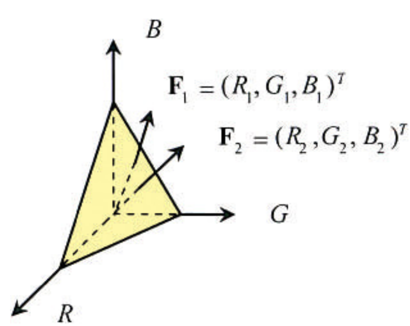

Figure 3.18. *Representation of two color vectors* $\mathbf{F}_1$ *and* $\mathbf{F}_2$ *in the RGB space.*

$$\Delta_I = |I_1 - I_2| \text{ and } \Delta_C = \sqrt{S_1^2 + S_2^2 - 2S_1S_2\cos\theta}\,,$$

whereby applies

$$\theta = \begin{cases} |H_1 - H_2| & \text{if } |H_1 - H_2| \le \pi \\ 2\pi - |H_1 - H_2| & \text{if } |H_1 - H_2| > \pi \end{cases}.$$

3.5.3 Color Difference Formulas in the CIELAB and CIELUV Color Spaces

According to Schrödinger [Sch20], it is generally accepted that the area of color appearance possesses a Riemann metric. The uniform color spaces represented can be used for this, using the Riemann metric as an adequate aid due to the approximately equal distance. However, this is reasonably possible only if the color-mapping behavior in the image-formation process can be related to the standard color system. This is the subject of Section 4.5.4 (calibration in the standard color system).

In the CIELAB and CIELUV color spaces the Euclidian distance is used for determining color distance (according to DIN 6174). The following applies:

$$\Delta E^*_{ab} = \sqrt{\Delta L^* \cdot \Delta L^* + \Delta a^* \cdot \Delta a^* + \Delta b^* \cdot \Delta b^*}$$

and (3.17)

$$\Delta E^*_{uv} = \sqrt{\Delta L^* \cdot \Delta L^* + \Delta u^* \cdot \Delta u^* + \Delta v^* \cdot \Delta v^*}\ .$$

The color difference ΔE^*_{ab} is used, for example, in object classification [Tom90] and the color difference ΔE^*_{uv} in color calibration. The formula for the CIELAB space is to be applied especially to body colors.

For typical applications in the printing industry, Stamm [Sta81] gives justifiable CIELAB color differences from a mean of six units with a standard deviation of around three to four units. In [Hal89], color surfaces and their color differences are represented in CIELAB units. Through this a rough impression for the estimation of CIELAB units can be won. Color distortions are possible, however, through the reproduction of color on paper. The data concerning the number of CIELUV units ΔE^*_{ab} and ΔE^*_{uv}, which by "juxtaposition" comparison of single colors are still distinguishable to the human eye under controlled viewing conditions (*JND, just noticeable difference*), varies between one unit [Sto et al. 88] and five units [Dal88].

Note that the color difference formulas described here are valid in general only for small color differences [Ric81]. In addition, the color differences are no longer valid under changed lighting conditions. The color difference measurements are designed above all for the dye industry, so that a transfer to color image processing is not automatically useful. Furthermore, their applicability in color image processing has not yet been sufficiently researched. These characteristics are sometimes not given adequate attention in publications dealing with color image processing.

Color differences can also be described by means of L^*-lightness, hue angle, and chroma. The following applies:

$$\Delta E_{ab}^* = \sqrt{\Delta L^* \cdot \Delta L^* + \Delta h_{ab}^* \cdot \Delta h_{ab}^* + \Delta C_{ab}^* \cdot \Delta C_{ab}^*}$$

and (3.18)

$$\Delta E_{uv}^* = \sqrt{\Delta L^* \cdot \Delta L^* + \Delta h_{uv}^* \cdot \Delta h_{uv}^* + \Delta C_{uv}^* \cdot \Delta C_{uv}^*}\,.$$

Likewise, it can be useful, for more exact specification, to examine a difference triplet $(\Delta L^*, \Delta C^*, \Delta H^*)$ of L^*-lightness, chroma, and hue angle in the respective color space. The hue angle difference is calculated from ΔE_{ab}^* and ΔE_{uv}^* with

$$\Delta H_{ab}^* = \sqrt{\Delta E_{ab}^* \cdot \Delta E_{ab}^* - \Delta L^* \cdot \Delta L^* - \Delta C_{ab}^* \cdot \Delta C_{ab}^*}$$

and (3.19)

$$\Delta H_{uv}^* = \sqrt{\Delta E_{uv}^* \cdot \Delta E_{uv}^* - \Delta L^* \cdot \Delta L^* - \Delta C_{uv}^* \cdot \Delta C_{uv}^*}\,.$$

The difference of the hue angle has a plus sign if the angle increases; otherwise it has a minus sign. A number of additional color difference formulas can be found, for example, in [Ber94], [Hun91], [Ric81] and [WysSti82]. A recent one for CIELAB is the CIE 2000 color difference formula CIDE2000 that can be found in [Luo et al. 01] together with a comparison of different color formulas for the CIELAB.

3.6 COLOR ORDERING SYSTEMS

The colors to characterize were described in the preceding sections through a set of numbers. This numeric systematization is often not suitable for the daily contact with colors, for by changing the number values every person makes an entirely individual conception of color. This fact has no great importance during the automatic segmentation of a color image in regions. In contrast, the classification of materials or the recognition of objects in color images can be supported considerably by the use of reference systems. Apart from the wealth of trade-specific color references there exist also a number of nationally and internationally standardized catalogs called *color ordering systems*. In color image processing they are used above all in colorimetric and photometric calibration. In the following sections, the Munsell Color System, the Macbeth ColorChecker, and the DIN colormap are described.

3.6.1 Munsell Color System

The Munsell Color System, developed by A.H. Munsell in 1905, found frequent distribution. Each of the over 1000 defined matte color planes are described by the three ordering attributes *hue H*, lightness *value V*, and *chroma C*. The hues are arranged in a circle that is separated into 100 perceptually equidistant steps with five principal hues and five intermediate-positioned hue steps. The principal and intermediate hues are indicated by red, yellow-red, yellow, green-yellow, green, blue-green, blue, purple-blue, purple, and purple-red. The lightness value is subdivided according to sensitivity into 11 equidistant gray shades. In this case, "absolute white" is indicated as "10/" and "absolute black" as "0/". The value "5/" lies, according to sensitivity, exactly in between and is indicated as a "middle gray."

The chroma has a resolution dependent on the hue. Its notation indicates the degree of divergence of a given hue from a neutral gray of the same value. the value "/0" indicates an absolute desaturation of color. The maxima lie by 10 to 14 and are even higher in some colors. A chromatic color is clearly referenced by the notation "*H V/C*" and an achromatic color by "*N V/*." Therefore, for example, *N* 8/ corresponds to a light gray, 5*YR* 7/12 a "rich" orange, and 5*R* 8/4 a "soft" pink. A transformation of *RGB* values into the Munsell notation is explained in [Tom87].

3.6.2 Macbeth ColorChecker

The Macbeth ColorChecker is frequently used in English-speaking countries for the calibration of color image processing systems (see Section 4.5.2). It concerns a reference map, which contains 24 matte color surfaces, used for the purpose of color evaluation. The 24 color surfaces comprise the primary colors of the additive and subtractive color mixture (see Section 2.2) as well as six achromatic colors (gray shades). The remaining colors adapt to our environment. For example, a leaf color, two skin colors, and several sky colors are included on the chart (see Fig. 3.19). The CIE coordinates x, y, Y and the Munsell notation are given for each color surface are presented in Table 3.2, where the xy coordinates relate to the standard illuminant C (see Fig. 4.2.2). The spectral reflection factors were represented graphically in [McC et al. 76] and in [Mey88].

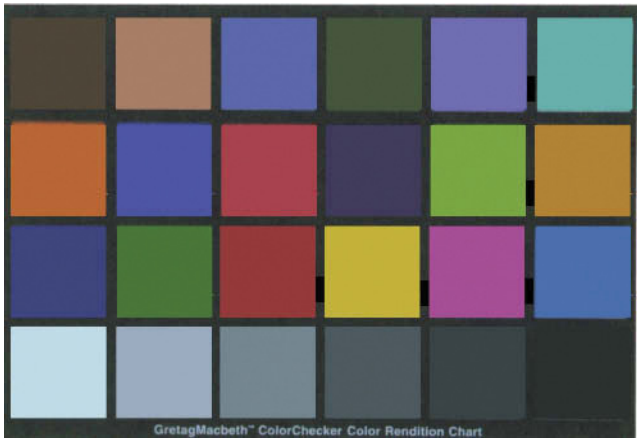

Figure 3.19. *Color image of the MacbethTM ColorChecker.*

3YR 3.7/3.2 Dark Skin	2.2YR 6.47/4.1 Light Skin	4.3PB 4.95/5.5 Blue Sky	6.7GY 4.2/4.1 Foliage	9.7PB 5.4/6.7 Blue Flower	2.5BG 7/6 Bluish Green
5YR 6/11 Orange	7.5PB 4/10 Purplish Blue	2.5R 5/10 Moderate Red	5P 3/7 Purple	5GY 7.1/9.1 Yellow Green	10YR 7/10 Orange Yellow
7.5PB 2.9/12.7 Blue	0.25G 5.4/8.65 Green	5R 4/12 Red	5Y 8/11.1 Yellow	2.5RP 5/12 Magenta	5B 5.08/8.0 Cyan
N 9.5/ White	N 8/ Gray	N 6.5/ Gray	N 5/ Gray	N 3.5/ Gray	N 2/ Black

Table 3.2. *The color or gray-level denotations and the Munsell denotations for the corresponding standardized color patches of the Macbeth ColorChecker.*

3.6.3 DIN Color Map

The German ordering system for body colors is the DIN colormap in accordance with DIN 6164. *Hue*, *saturation*, and *lightness* form the ordering features in the DIN color system. These terms were chosen because they correspond to a very natural description of the sensitivity of a color impression.

Hue	Number
Yellow	1
Red	7
Blue	16
Green	22

Table 3.3. *DIN6164 hue numbers.*

The color identification results from the hue number T, the degree of saturation S, and the degree of darkness D with the notation $T : S : D$. The hues are subdivided into 24 parts on a circle (see Table 3.3). For achromatic colors, an N is noted for the hue number. In contrast to the Munsell system, the saturation lines, in relation to the standard color table, remain equal with the lightness and lie on straight lines that pass through the origin. The fundamental characteristic of this system is the equal distance according to the sensitivity of the individually defined color rows.

In addition to the DIN colormap, other DIN color models exist that were developed and standardized for the color quality control of color television transmissions and color film scanning (see DIN 6169).

3.7 FURTHER READING

A representation of color spaces from a computer graphics point of view is found in [Fol et al. 94] and a representation from the image processing point of view in [Pra91], [SanHor98], and [PlaVen00]. We recommend [Ber94] for an introduction to color metrics and color differences. The topic of color management is discussed in [Har01] and [GioMad98]. A very comprehensive description (976 pages) of color spaces and color difference measurements is given in [WysSti82].

Nowadays, the data for the CIE chromaticity diagram no longer needs to be copied from the data sheets of the lighting commission CIE. It is available at http://www-cvrl.ucsd.edu/ on the Internet. Beyond that, the homepage of the lighting commission CIE, http://www.cie.co.at/cie/home.html, contains additional interesting references to further data material. Information about *sRGB* is available at http://www.srgb.com. We refer to the newsgroup news:sci.engr.color for current discussions on color-related topics.

3.8 REFERENCES

[Ber94] A. Berger-Schunn. Practical Color Measurement: A Primer for the Beginner, a Reminder for the Expert. Wiley, New York, 1994.

[BroYan89] D.C. Brockelbank, Y.H. Yang. An experimental investigation in the use of color in computational stereopsis. *IEEE Transactions on Systems, Man, and Cybernetics* **19** (1989), pp. 1365-1383.

[ConFli97] C. Connolly, T. Fliess. A study of efficiency and accuracy in the transformation from RGB to CIELAB color space. *IEEE Transactions on Image Processing* **6** (1997), pp. 1046-1048.

[Dal88] C.J. Dalton. The measurement of the colorimetric fidelity of television cameras. *J. Inst. of Electronic and Radio Engineers* **58** (1988), pp.181-186.

[DIN 5033] Deutsche Normen. DIN 5033: *Farbmessung*, Teil 1-9, March 1979. [DIN 6174] Deutsche Normen. DIN 6174: Farbmetrische Bestimmung von Farbabständen bei Körperfarben nach der CIELAB-Formel. January 1979.

[Fol et al. 94] J.D. Foley, A. van Dam, S.K. Feiner, J.F. Hughes, R.L. Phillips. *Introduction to Computer Graphics*. Addison-Wesley, Reading, 1994.

[Fre88] H. Frey. *Digitale Bildverarbeitung in Farbräumen.* Doktorarbeit (Ph.D. Thesis), University Ulm, Germany, 1988.

[GioMad98] E.J. Giorgianni, T.E. Madden. *Digital Color Management: Encoding Solutions*. Prentice Hall, Englewood Cliffs, New Jersey, 1998.

[Hal89] R. Hall. Illumination and Color in Computer Generated Imagery. Springer, Berlin, Germany, 1989.

[Har01] J. Hardeberg. Acquisition and Reproduction of Color Images: Colorimetric and Multispectral Approaches. Universal, Parkland, Florida, 2001.

[Hol82] K. Holla. Opponent colors as a 2-dimenional feature within a model of the first stages of the human visual system. *Proc. 6th Int. Conference on Pattern Recognition*, Munich, Germany, 1982, pp. 561-563.

[Hun91] R.W.G. Hunt. *Measuring Colour.* Ellis Horwood, Chichester, Sussex, England, 1991.

[Luo96] M.R. Luo. The LLAB model for colour appearance and colour difference evaluation. *Proc. SPIE **2658**,* Color Imaging: Device-Independent Color, Color Hard Copy and Graphic Arts, San Jose, California, 1996, pp. 261-269.

[Luo et al. 01] M.R. Luo, G. Cui, B. Rigg. The development of the CIE 2000 colour-difference formula: CIDE2000. *Color Research & Application* **26** (2001), pp. 340-350.

[McC et al. 76] C.S. McCamy, H. Marcus, J.G. Davidson. A color-rendition chart. *J. Applied Photographic Engineering* **2** (1976), pp. 95-99.

[Mey88] G.W. Meyer. Wavelength selection for synthetic image generation. *Computer Vision, Graphics, and Image Processing* **41** (1988), pp. 57-79.

[MonFai97] E.D. Montag, M.D. Fairchild. Psychophysical evaluation of gamut mapping techniques using simple rendered images and artificial gamut boundaries. *IEEE Transactions on Image Processing* **6** (1997), pp. 977-989.

[Oht et al. 80] Y.-I. Ohta, T. Kanade, T. Sakai. Color information for region segmentation. *Computer Graphics and Image Processing* **13** (1980), pp. 222-241.

[PlaVen00] K.N. Plataniotis, A.N. Venetsanopoulos. *Color Image Processing and Applications*. Springer, Berlin, Germany, 2000.

[Poy96] C.A. Poynton:. *A Technical Introduction to Digital Video*. Wiley, New York, 1996.

[Poy97] C. Poynton. Poynton's color FAQ. WWW-Note at http://www.poynton.com/ColorFAQ.html, 1997.

[Pra91] W.K. Pratt. *Digital Image Processing*, 2nd ed., Wiley, New York, 1991.

[Ric81] M. Richter. *Einführung in die Farbmetrik*. 2nd ed., Walter de Gruyter, Berlin, 1981.

[SanHor98] S.J. Sangwine, R.E.N. Horne. *The Colour Image Processing Handbook*. Kluwer, Boston, 1998.

[Sch20] E. Schrödinger. Grundlagen einer Theorie der Farbmetrik im Tagessehen. *Ann. Physik (IV)* **63**, 1920, pp. 397-456, 489-520.

[Spa et al. 00] K.E. Spaulding, G.J. Woolfe, E.J. Giorgianni. Image states and standard color encodings (RIMM/ROMM RGB). *Proc. IS&T 8th Color Imaging Conference*, 2000, pp. 288-294.

[Sta81] S. Stamm. An investigation of color tolerance. *Technical Association of the Graphic Arts Conference*, 1981, pp. 157-173.

[Sto et al. 88] M.C. Stone, W.B. Cowan, J.C. Beatty. Color gamut mapping and the printing of digital color images. *ACM Transactions on Graphics* **7** (1988), pp. 249-292.

[Sto et al. 96] M. Stokes, M. Anderson, S. Chandrasekar, R. Motta. A standard default color space for the internet: sRGB, version 1.10, 1996 at http://www.color.org/sRGB.html.

[Süs et al. 99] S. Süsstrunk, R. Buckley, S. Sven. Standard RGB color spaces. *Proc. of IS&T/SID's 7th Color Imaging Conference*, 1999, pp. 127-134.

[Tom87] S. Tominaga. Expansion of color images using three perceptual attributes. *Pattern Recognition Letters* **6** (1987), pp. 77-85.

[Tom90] S. Tominaga. A color classification method for color images using a uniform color space. *Proc. 10th Int. Conference on Pattern Recognition*, Atlantic City, New Jersey, 1990, Vol. I, pp. 803-807.

[TruKul96] H.J. Trussell, M.S. Kulkarni. Sampling and processing of color signals. *IEEE Transactions on Image Processing* **5** (1996), pp. 677-681.

[TseCha92] D.-C. Tseng, C.-H. Chang. Color segmentation using perceptual attributes. *Proc. 11th Int. Conference on Pattern Recognition*, The Hague, the Netherlands, 1992, Vol. III, pp. 228-231.

[WysSti82] G. Wyszecki, W.S. Stiles. *Color Science: Concepts and Methods, Quantitative Data and Formulae*, 2nd ed., Wiley, New York, 1982 (also available in paperback, printed 2000).